J Incl Phenom Macrocycl Chem (2013) 75:47–56
DOI 10.1007/s10847-012-0145-5

ORIGINAL ARTICLE

Permethylated β-cyclodextrin/pesticide complexes: X-ray structures and thermogravimetric assessment of kinetic parameters for complex dissociation

Dyanne L. Cruickshank · Natalia M. Rougier · Vaughan J. Maurel · Rita H. de Rossi · Elba I. Buján · Susan A. Bourne · Mino R. Caira

Received: 7 February 2012 / Accepted: 7 March 2012 / Published online: 13 April 2012

Abstract The X-ray crystal structures of the inclusion complexes formed between three pesticides (two organophosphorus insecticides and one chloroacetanilide herbicide) and permethylated β-cyclodextrin (TRIMEB) are reported. The complexes TRIMEB–fenitrothion (**1**), TRIMEB–fenthion (**2**) and TRIMEB–acetochlor (**3**) are members of a commonly occurring isostructural series. The mode of inclusion of the two organophosphate insecticides is very similar, while the acetochlor molecule, which is structurally quite distinct from the two insecticide molecules, adopts a somewhat different position within the TRIMEB cavity. In addition to the structural elucidation of these complexes, their thermal behaviour was investigated using isothermal and non-isothermal thermogravimetry. The isothermal results showed that the dissociation of the guest molecules from the TRIMEB cavities can best be described by two mechanisms, namely a first-order reaction model and a three-dimensional diffusion model. Both the isothermal and non-isothermal methods allowed the determination of the activation energies of the guest loss process for each complex.

Keywords Pesticides · Inclusion complexes · Permethylated β-cyclodextrin · Single crystal X-ray diffraction · Thermal decomposition kinetics

Introduction

The ability of cyclodextrins (CDs) to form inclusion complexes with various guest molecules has been studied extensively over the last few decades especially within the pharmaceutical industry, as well as the food, cosmetic and biotechnology industries, and in the field of analytical chemistry [1]. In 1985 Szejtli [2] reviewed the subject of CDs and pesticides, stating that within the next decade, there would be a rapid development in the application of CDs in pesticide formulations accompanying the decrease in the price of CDs and the increasing rate of CD production. Since then the focus has been on studying the interactions between pesticides and CDs in solution as well as in the solid state and evaluating the possible benefits that could be conferred on pesticides upon their complexation with biodegradable host molecules such as CDs. In general, the undesirable physicochemical properties associated with pesticides include their poor aqueous solubility, chemical, thermal and physical instability, high volatility, high soil mobility and poor wettability [3].

The three pesticides selected for this study are the insecticides fenitrothion [*O*,*O*-dimethyl *O*-(3-methyl-4-nitrophenyl) phosphorothioate] and fenthion [*O*,*O*-dimethyl *O*-[3-methyl-4-(methylthio)phenyl] phosphorothioate], and the herbicide acetochlor [2-chloro-*N*-(ethoxymethyl)-*N*-(2-ethyl-6-methylphenyl)acetamide] (Fig. 1). These compounds are oils at room temperature and are currently registered for use in several countries [4]. The reduced chemical and thermal stability of these pesticides, as well as the difficulties

Electronic supplementary material The online version of this article (doi:10.1007/s10847-012-0145-5) contains supplementary material, which is available to authorized users.

D. L. Cruickshank · V. J. Maurel · S. A. Bourne · M. R. Caira (✉)
Department of Chemistry, University of Cape Town, Rondebosch 7701, South Africa
e-mail: mino.caira@uct.ac.za

N. M. Rougier · R. H. de Rossi · E. I. Buján
Instituto de Investigaciones en Físico Química de Córdoba (INFIQC), Departamento de Química Orgánica, Facultad de Ciencias Químicas, Universidad Nacional de Córdoba, Ciudad Universitaria, X5000HUA Córdoba, Argentina

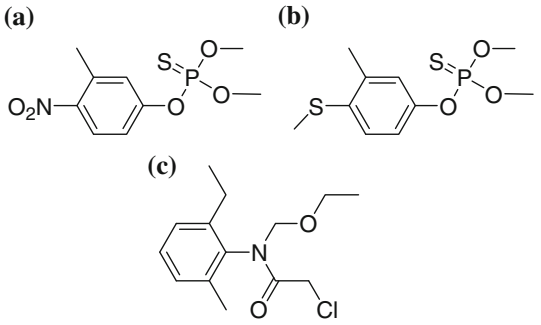

Fig. 1 The chemical structures of **a** fenitrothion, **b** fenthion and **c** acetochlor

associated with their handling and transportation, make them ideal candidates for solid-state formulation prior to application.

Previous studies of the stability of the organophosphate insecticides fenitrothion and fenthion have shown that the native CDs have a catalytic effect on the photodegradation rate of these pesticides in humic water [5]. However, other investigations have shown that CDs induce an inhibitory effect on the degradation of fenitrothion in basic media [6, 7]. No studies on the complexation of the chloroacetanilide herbicide acetochlor with CDs in the solid state or in solution have hitherto appeared in the literature.

Recently we reported the ability of fenitrothion to form solid inclusion complexes with both hexakis(2,3,6-tri-*O*-methyl)-α-CD (TRIMEA) and heptakis(2,3,6-tri-*O*-methyl)-*β*-CD (TRIMEB) [8]. We have since generated two additional TRIMEB complexes with guests fenthion and acetochlor which are isostructural with the TRIMEB–fenitrothion complex. In this paper, the similarities and differences amongst these three structures will be discussed and an attempt made to reconcile the crystal structures and the results obtained from the isothermal and non-isothermal kinetic experiments. The activation energies of complex dissociation obtained from the solid-state kinetic experiments will provide an indication of the thermal stability conferred upon the guest molecules by their encapsulation within CD molecules.

Experimental

Materials and solid complex preparation

The host compound heptakis(2,3,6-tri-*O*-methyl)-*β*-CD (TRIMEB) was purchased from Cyclolab (Budapest, Hungary) and was used as received. Fenitrothion was isolated as a yellow oil from a commercial sample of Sumithion (Sumitomo Chemical, NY, USA) by column chromatography over silica gel and was characterized by ^{1}H and ^{31}P NMR spectroscopy and GC–MS. The agrochemicals fenthion and acetochlor were obtained from Sigma Aldrich (Germany) and ChemService (USA) respectively.

Single crystals of each inclusion complex were prepared using the method of co-precipitation. Preparative details for TRIMEB–fenitrothion (**1**) were reported previously [8]. For the preparation of the inclusion complex TRIMEB–fenthion (**2**), 119 mg of TRIMEB (0.083 mmol) was weighed into a vial and 2 cm^3 of distilled water was added. An equimolar quantity (23 mg, 0.083 mmol) of the insecticide fenthion was added and the suspension was stirred for 4 h between 0 and 4 °C. The final clear solution was then filtered through a 0.45 μm filter into a clean vial and placed in an oven at 60 °C. The TRIMEB–acetochlor (**3**) inclusion complex was prepared by dissolving 106 mg (0.074 mmol) of the host in 5 cm^3 of distilled water at room temperature, and adding to the solution an equimolar quantity of acetochlor (20 mg, 0.074 mmol). The resulting suspension was stirred for 8 h and filtered into a clean vial which was also placed in an oven set at 60 °C. Single crystals of **2** and **3** appeared within 24 h.

The samples used for the solid-state kinetic studies were prepared by mechanical grinding of equimolar quantities of the host and guest in a mortar for 30 min in the absence of water. The mass of the guest was kept constant at 20 mg and the mass of TRIMEB varied depending on the molecular weight of each guest compound. The particle size distributions of the samples were measured using a Multisizer^{TM} 3 Coulter Counter. The mechanical co-grinding method yielded samples with particle diameters in the range 20–45 μm, with a mean diameter of ca. 25 μm.

Single crystal X-ray diffraction

X-ray structural elucidation of complex **1** was described earlier [8]. Intensity data-collection for complexes **2** and **3** were performed on a Bruker KAPPA APEX II DUO diffractometer. The crystals were maintained at 100(2) K throughout the data-collection using Cryostream coolers (Oxford Cryosystems UK). Unit cell refinements and data reductions were performed using the program SAINT [9]. For both complexes **2** and **3**, the Laue system was found to be *mmm*, indicating the orthorhombic crystal system and the common space group $P2_12_12_1$ was uniquely identified from systematic absences. Data were corrected for Lorentz-polarization effects and for absorption (program SADABS [10]). Structure solution for complexes **2** and **3** was achieved by using the host atomic coordinates of the isostructural complexes TRIMEB–*p*-iodophenol [11] and TRIMEB–ethyl laurate [12] respectively, as trial models. All non-hydrogen atoms, except O6, C7, C8 and C9 of each methyl glucose unit, served as the input model. The structures were refined with SHELXH-97 [13] and successive difference Fourier maps revealed the methoxyl groups and guest molecules. All non-hydrogen atoms of complex **2** were refined anisotropically except for one of the primary methoxyl carbon atoms of

the host, which had a reasonable isotropic thermal parameter but an unacceptable thermal ellipsoid when refined anisotropically. For complex **3**, one primary methoxyl group of the host molecule was disordered over two positions, as were atoms C17A and Cl18 of the guest molecule. This disorder was modelled by allowing the two components in each case to refine isotropically with site-occupancy factors x and $1 - x$. The final value of x refined to 0.65 and 0.57 for the major components of the host and guest atoms respectively. All ordered atoms of complex **3** were refined anisotropically. Although some of the guest H atoms were apparent in the difference Fourier maps for complexes **2** and **3** all the H atoms were added in idealised positions in a riding model with U_{iso} values 1.2–1.5 times those of their parent atoms.

Powder X-ray diffraction (PXRD)

PXRD patterns were recorded at room temperature using a Huber Imaging Plate Guinier Camera 670 with nickel-filtered CuKα_1 radiation ($\lambda = 1.5405981$ Å) produced at 40 kV and 20 mA by a Philips PW1120/00 generator. A 2θ range of 4–100° was used with a step size of 0.005° 2θ. The samples were exposed to the X-ray beam for 30 min with 10 multi-scans to collect the data.

Thermal analysis

Thermogravimetric analysis (TGA) and differential scanning calorimetric (DSC) measurements were performed using TA instruments (TA-Q500 and DSC-Q200) with Universal Analysis 2000 software. The TG instrument operated with dry nitrogen purge gas flowing at a rate of 60 cm^3 min^{-1} while the DSC operated with a flow rate of 50 cm^3 min^{-1}. For consistency, the sample size for each isothermal and non-isothermal TG run was kept small and relatively constant (1.77–1.94 mg). For each TG experiment the complex material (**1**, **2** or **3**) was placed in an open aluminium pan and a specific temperature program was applied. DSC measurements were conducted in closed aluminium pans.

Isothermal TG runs were performed by heating the sample at a rate of 30 or 40 K min^{-1} to a specific temperature which was then maintained for 300 min. The non-isothermal (dynamic) TG experiments were performed by heating the powdered samples from 20 to 300 °C at different heating rates (1.0, 2.5, 5.0, 7.5 and 10.0 K min^{-1}).

Results and discussion

Single crystal X-ray structures

Table 1 lists crystal data and refinement details for complexes **1**, **2** and **3**. The three complexes are isostructural as is evident from the close similarity in their unit cell dimensions and the identical space group ($P2_12_12_1$) in which they crystallize. The X-ray crystal structure of **1** has been described in detail previously [8]; however, for comparison the monomeric units of complexes **1**, **2** and **3** are shown in Fig. 2, which views them from a common direction. The dimethyl phosphorothioate units of fenitrothion and fenthion in complexes **1** and **2** are situated close to the primary rims of the TRIMEB cavities which are blocked by several methoxyl groups in each case. The 3-methyl and 4-methylsulfanyl groups positioned on the aromatic ring in complex **2** protrude from the secondary rim of the TRIMEB cavity into the interstitial spaces between neighbouring TRIMEB molecules. This particular location of the aromatic substituents is similar to that in complex **1**.

When compared with the modes of inclusion of the organophosphate insecticide guest molecules, the acetochlor molecule assumes a different position and orientation within the TRIMEB cavity (Fig. 2c). The aromatic moiety is fully encapsulated by the host molecule, while the ethyl substituent and chloro-ethoxymethyl acetamide group of acetochlor extend from the secondary rim of the TRIMEB cavity. The primary rim is once again 'sealed off' by the primary methoxyl groups which fold over giving the TRIMEB host molecule a cup-like shape. There are no hydrogen bonds between the acetochlor and TRIMEB molecules. Several intramolecular and intermolecular host–host interactions of the type C–H···O exist in all three complex structures. These hydrogen bonds are essential in maintaining the overall framework of the crystal structure.

The X-ray structures of **2** and **3** provide the first accurate representations of the fenthion and acetochlor molecules in the solid state. It is important to note the geometry of each guest. The dimethyl phosphorothioate unit of fenthion adopts the usual tetrahedral conformation and the 4-methylsulfanyl group displays a slight twist out of the plane of the aromatic ring (the dihedral angle C–C-S–C is 24.1(7)°). For acetochlor, the angle between the least-squares plane through the acetamide group (C_2N–C=O) and the phenyl ring plane is 85.4(3)°. This value is similar to that observed in the crystal structure of an intermediate used for the synthesis of acetochlor, namely 78.0(3)° [14]. All other geometrical parameters for the fenthion and acetochlor molecules are in the expected ranges.

Geometrical parameters for the host molecule in complexes **2** and **3** are comparable to those observed in complex **1** [8] and in several other isostructural TRIMEB complexes [15]. Figure 3 illustrates the packing arrangement for complex **2** as representative. The complex units pack in a screw-channel mode and are arranged in a head-to-tail manner parallel to the b-axis. This diagram shows that the guest molecules are isolated from one another. The

Table 1 Crystal data and structure refinement for the complexes **1** [8], **2** and **3**

	1	**2**	**3**
Chemical formula	$C_{63}H_{112}O_{35}{\cdot}C_9H_{12}NO_5PS$	$C_{63}H_{112}O_{35}{\cdot}C_{10}H_{15}O_3PS_2$	$C_{63}H_{112}O_{35}{\cdot}C_{14}H_{20}ClNO_2$
Formula weight	1706.75	1707.84	1699.29
Crystal system	Orthorhombic	Orthorhombic	Orthorhombic
Unit cell constants			
Space group	$P2_12_12_1$	$P2_12_12_1$	$P2_12_12_1$
a (Å)	15.1588(4)	15.084(2)	14.728(2)
b (Å)	21.1279(4)	21.164(3)	21.542(3)
c (Å)	27.5575(7)	27.491(3)	27.604(4)
$\alpha = \beta = \gamma$ (°)	90	90	90
Volume (Å^3)/Z	8825.9(4)/4	8,776(2)/4	8,758(2)/4
Density$_{(calc)}$ (g cm^{-3})	1.284	1.293	1.289
Temperature (K)	173(2)	100(2)	100(2)
Wavelength (Å)	0.71073	0.71073	0.71073
Dimensions (mm)	0.24 × 0.13 × 0.11	0.30 × 0.12 × 0.05	0.30 × 0.27 × 0.07
θ-range collection (°)	2.69–25.70	1.48–24.75	1.83–25.87
Index range	$-18 \le h \le 18$	$-9 \le h \le 17$	$-17 \le h \le 15$
	$-25 \le k \le 25$	$-25 \le k \le 25$	$-26 \le k \le 22$
	$-33 \le l \le 33$	$-32 \le l \le 32$	$-29 \le l \le 33$
Reflections collected	121,751	73,115	55,784
Independent reflections	16,732	8,481	9,159
Reflections with $I > 2\sigma(I)$	11,175	6,530	6,877
Number of parameters	959	1,026	1,034
R_{int}	0.0568	0.0459	0.0485
Goodness of fit	1.021	0.977	1.025
R_1 [$I > 2\sigma(I)$]	0.0626	0.0519	0.0540
wR_2	0.1428	0.1316	0.1301
Largest difference peak and hole (e Å^{-3})	0.71/−0.74	0.64/−0.60	0.92/−0.69

isostructurality of complexes **1**, **2** and **3** implies a common arrangement of the host molecules and thus the packing arrangements of the complex units are identical. This is evident from the experimental PXRD patterns of the three complexes that were obtained by kneading (Fig. 4). These patterns are also consistent with the corresponding computed patterns (see supporting information), confirming that the single crystals selected for X-ray analyses are representative of the respective bulk materials. A detailed comparison of the computed patterns for complexes **1** and **2**, containing guests that are close analogues, shows the patterns to be in very good correspondence. Significant intensity differences arise for **3**, owing to the different nature of the included acetochlor molecule and its unique location in the host cavity.

Thermal analysis

Thermal profiles

The TG traces for the three TRIMEB inclusion complexes all display two-step mass losses. The first one corresponds to a single guest molecule being released from the CD cavity [exptl. 16.5 ± 0.1, 16.5 ± 0.2 and 16.3 ± 0.2 % ($n = 5$); calcd. for a 1:1 host–guest ratio, 16.2, 16.3 and 15.9 % for complexes **1**, **2** and **3**, respectively] and the second mass loss can be attributed to host decomposition (Fig. 5). There was a considerable difference in the onset temperatures of guest loss for the samples prepared by co-grinding (see supporting information) vis-à-vis those prepared by co-precipitation, on which the crystal structure determinations were based. These

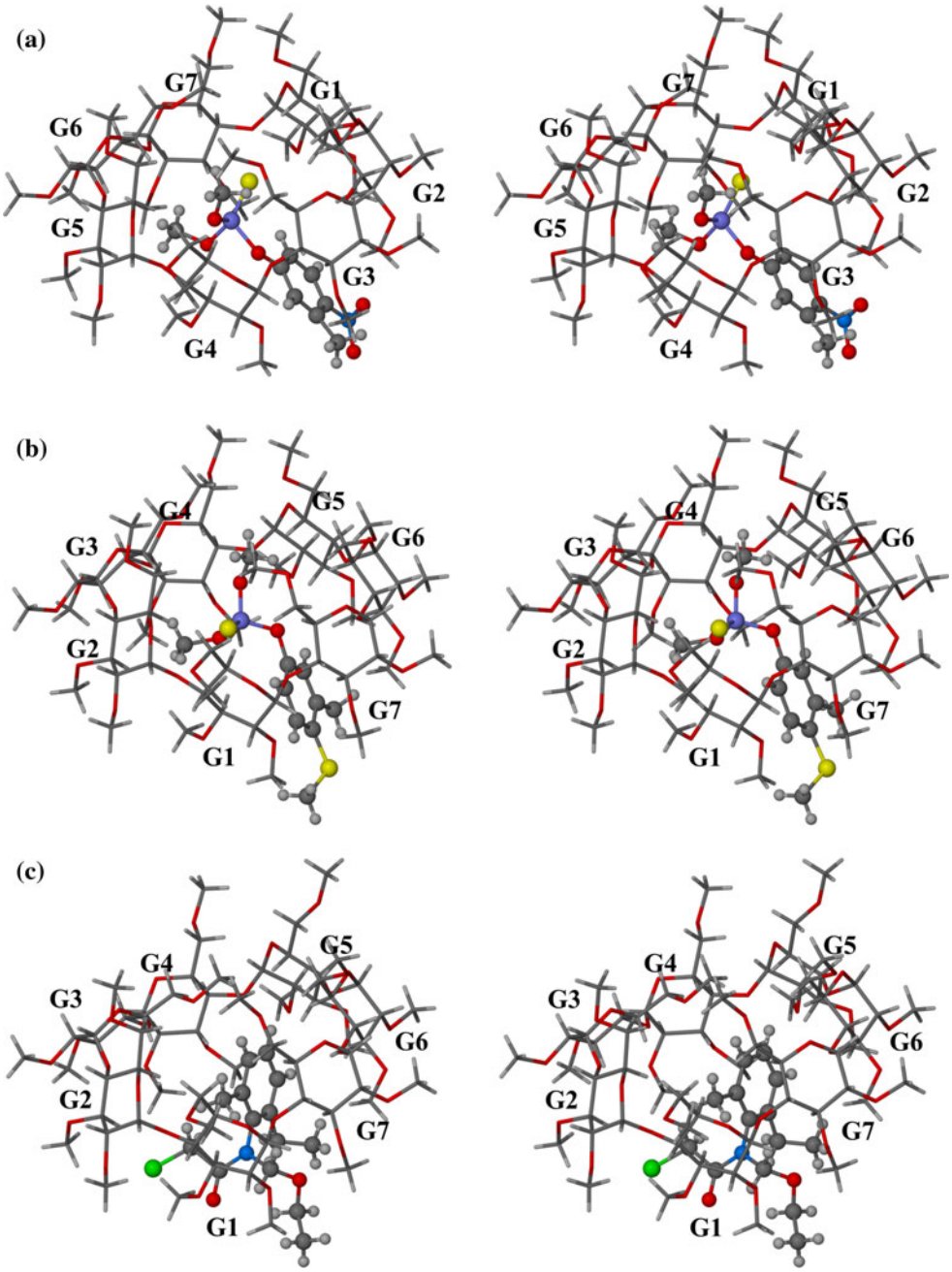

Fig. 2 Stereoviews of the complexes **1**, **2** and **3** with their host residue numbering. For clarity, only the major host and guest components of complex **3** are shown

differences have been summarised in Table 2 and are a result of the different average particle sizes of each sample. The co-precipitation method produced large single crystals that were gently crushed and blotted dry on filter paper before being placed in the TG instrument, whereas the materials obtained by kneading contained particles of smaller average size, resulting in guest loss occurring at a lower temperature. The melting points of the complexes (as determined by DSC) prepared by the two methods differ by a maximum of only 3 K. This minimal temperature difference is due to the excellent heat transference between the closed sample pans and the thermoelectric discs on which the pans are positioned.

Despite the early onset temperatures at which guest loss for the complexes commences, the entire process of guest loss takes place over a wide temperature range (onset temp. to ~240 °C). Consequently, the processes of guest loss and complex fusion partially overlap, guest loss preceding fusion in each case.

Isothermal method

The general equation used to study the kinetics of a solid-state process at a constant temperature can be represented by Eq. 1 or by the integral form (Eq. 2),

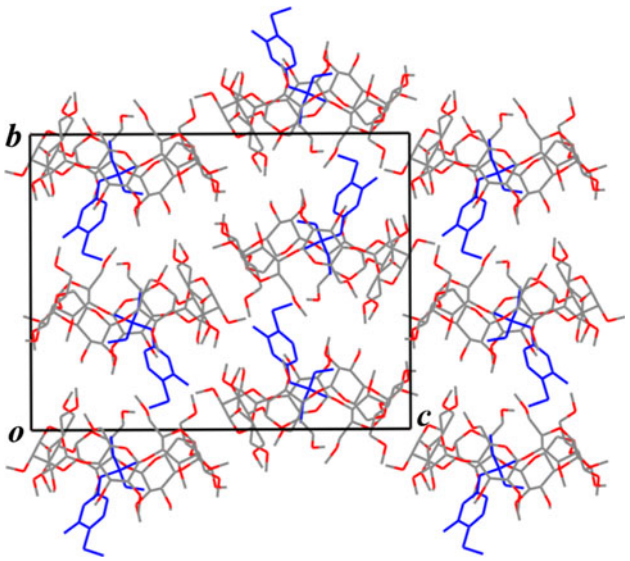

Fig. 3 A packing diagram of complex **2** viewed along [100]. Hydrogen atoms have been omitted for clarity

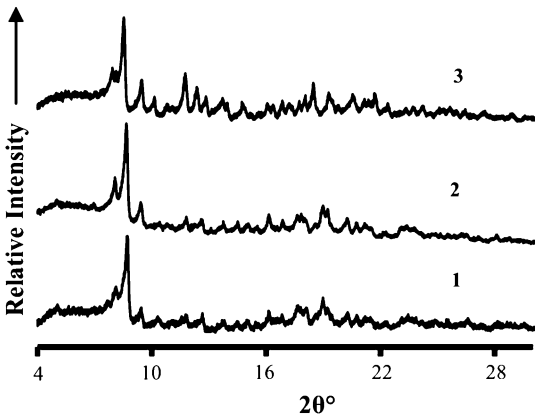

Fig. 4 Experimental PXRD patterns of the three isostructural complexes obtained by kneading TRIMEB and the respective guests. These patterns match those generated from the single crystal X-ray data (see supporting information)

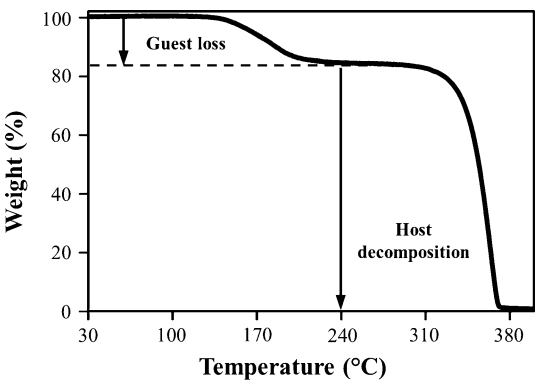

Fig. 5 A schematic TG trace for the TRIMEB inclusion complexes **1–3**

$$\frac{d\alpha}{dt} = kf(\alpha) \quad (1)$$

$$g(\alpha) = kt \quad (2)$$

where α is the fractional mass loss $[(m_t - m_o)/(m_\infty - m_o)]$ at reaction time t, k is the rate constant and $f(\alpha)$ and $g(\alpha)$ are functions that describe a particular reaction mechanism. The α-time curves obtained from the isothermal experiments conducted for each complex are shown in Fig. 6. These plots show deceleratory behaviour and were analysed using various mathematical expressions derived from proposed mechanisms for a range of solid-state processes [16]. For our results, the equation based on the first-order reaction model (F1, Eq. 3) as well as the equation based on the 3-D diffusion model (3D, Eq. 4), showed a high degree of linearity and good correlation coefficients when fitted to the α versus time graphs over an α range of 0.0–0.8 for the F1 model and 0.1–0.9 for the 3D model.

$$-\ln(1-\alpha) = kt \quad (3)$$

$$\left[1-(1-\alpha)^{1/3}\right]^2 = kt. \quad (4)$$

Using both models we were able to obtain two sets of rate constants (k) at specific temperatures for each complex studied. An Arrhenius plot ($\ln k$ vs. $1/T$) provided a straight line (Fig. 7), from which the activation energy (Table 3) associated could be determined. We interpret the derived E_a values here as referring to the composite process of guest loss and complex fusion owing to the wide α-ranges spanned in the isothermal experiments.

There are many instances in the literature where more than one solid-state model can be used to describe a particular process [17, 18]. The F1 model is based on the apparent 'order' of reaction as seen for rate laws established in solution; however, it does not have the same significance for solid-state reactions. The mechanism of a first-order reaction involves random nucleation (either at a particle surface or at an imperfection) and growth of these nucleation sites that does not advance beyond the individual crystallite nucleated [16]. The activation energies obtained using this model (Table 3) are not statistically different, suggesting that the kinetics of the process of guest loss and melting of a given complex is not dependent on the structure of the guest molecule within the TRIMEB cavity.

The 3D model applies to a diffusion-limited reaction which takes place at a phase interface that forms between the product (TRIMEB) and the reactant (TRIMEB–pesticide complex). During the process of dissociation, the guest molecules diffuse towards the crystal surface and finally desorb from the surface. The activation energies obtained from the 3D model (Table 3) are very similar once again but do display a decreasing trend. One can

Table 2 The onset temperatures of guest loss and the melting points of the three complexes prepared using two methods

Complex	Onset temperature of guest loss as determined by TGA (°C)[a]		Temperature of complex fusion determined by DSC (°C)	
	Co-precipitation	Co-grinding	Co-precipitation	Co-grinding[b]
1	129	100	160	158
2	135	93	153	152
3	109	83	136	133

[a] These temperatures were measured based on the standard 10 K min^{-1} heating rate

[b] See Supplementary data for the DSC profiles

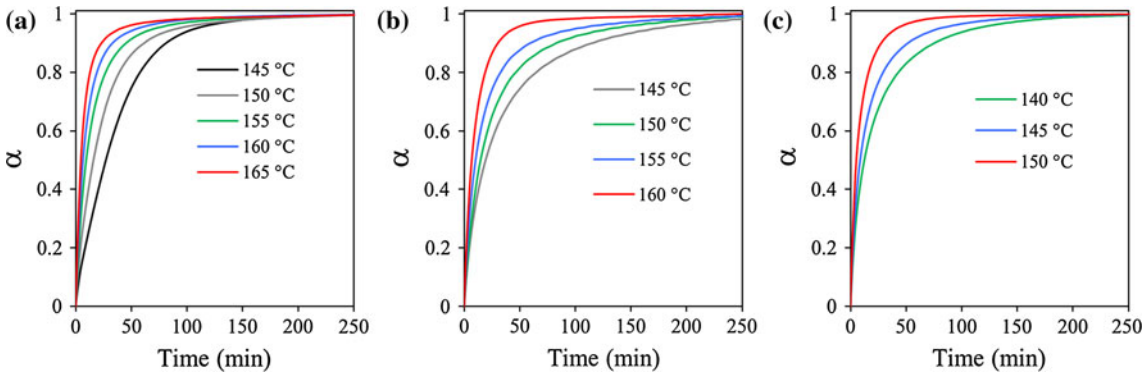

Fig. 6 Isothermal plots of α versus time for complexes **a 1**, **b 2** and **c 3**

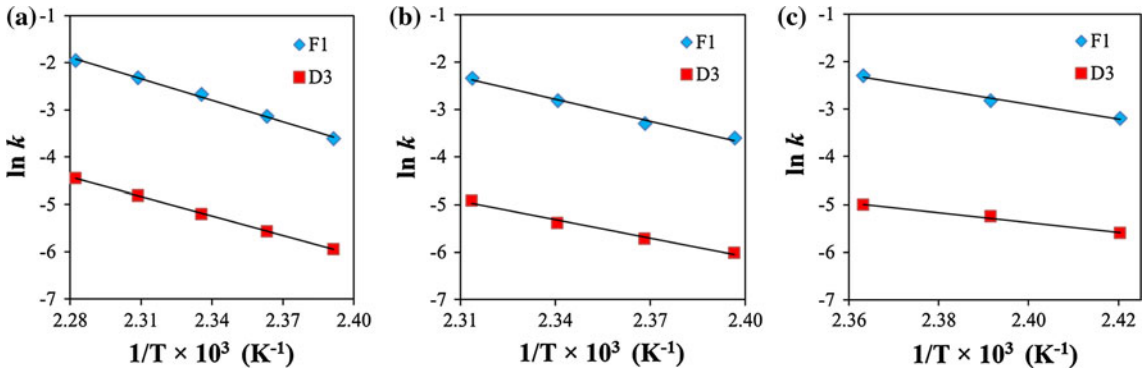

Fig. 7 Arrhenius plots obtained from the isothermal kinetic data for **a 1**, **b 2** and **c 3**

Table 3 Activation energies determined from the isothermal experiments for each complex using the two best-fitting models (F1 and 3D)

	1		**2**		**3**	
	F1	3D	F1	3D	F1	3D
E_a (kJ mol^{-1})	126 ± 4	114 ± 1	129 ± 10	109 ± 9	130 ± 13	86 ± 8
r^2	0.997	0.999	0.989	0.986	0.990	0.991

therefore propose that the kinetics of the process is dependent on the structure or physical properties of the complexes, e.g. their melting points (decreasing in the order **1** > **2** > **3**). Even though the guest loss process being studied is complicated due to two simultaneous events occurring (guest loss and complex fusion), the 3D model appears to be a reasonable one to be applied to the kinetics of the above events. Prior to the complexes melting, the 3D model is consistent with the crystal packing arrangement of the complexes. The guest molecules pack within their respective TRIMEB crystal structures such that they are isolated from one another and there are no particular directional constraints on their diffusion (Fig. 8).

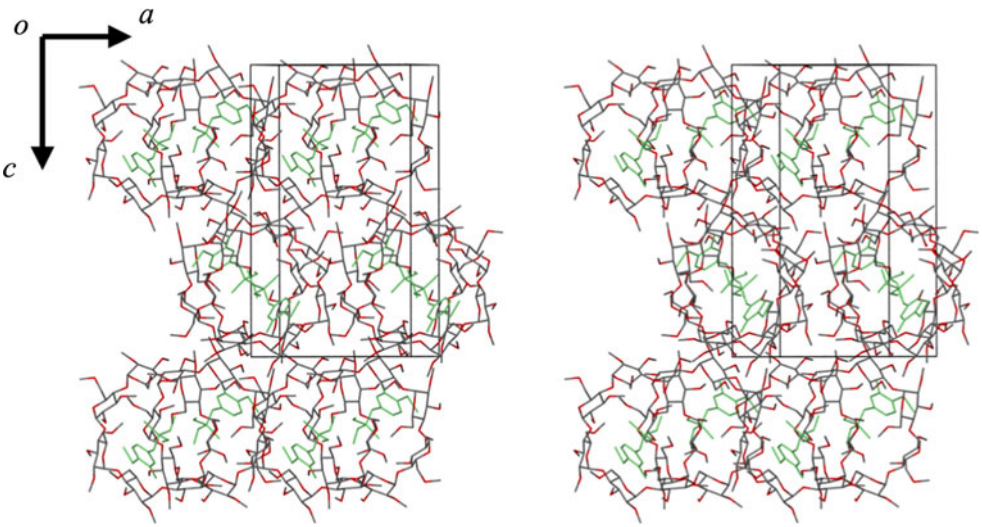

Fig. 8 A stereoview showing the packing in the crystal of complex **2** viewed along the *b*-axis to illustrate the lack of continuous channels. Hydrogen atoms have been omitted for clarity

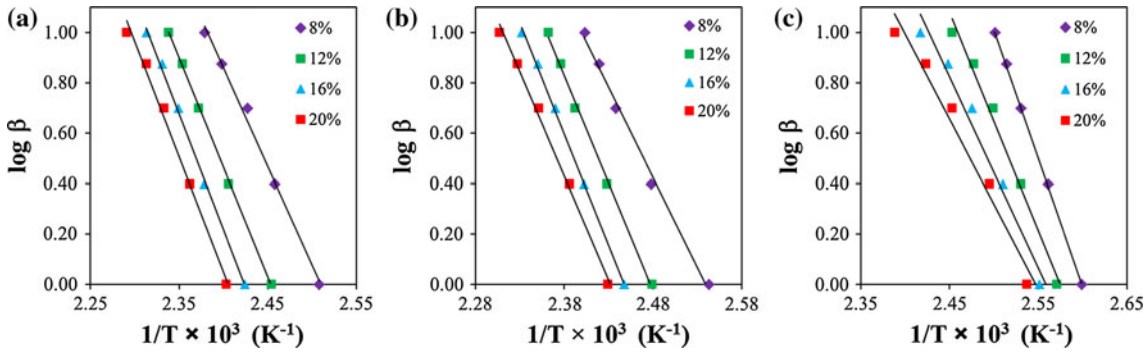

Fig. 9 Plots of log β versus $1/T$ for complexes **a 1**, **b 2** and **c 3**

Non-isothermal method

A model-free isoconversional method based on the Ozawa, Flynn and Wall (OFW) method [19, 20] was used to determine the activation energies for comparison with those obtained from the isothermal experiments performed on the three isostructural complexes. Equation 5 allowed the determination of the activation energies at each conversion level, where β_α is the heating rate, A_α the frequency factor, $E_{a\alpha}$ is the activation energy, T_α is the temperature at each conversion level and $g(\alpha)$ refers to the kinetic model.

$$\log\beta_\alpha = \log\frac{A_\alpha E_{a\alpha}}{g(\alpha)R} - 2.315 - 0.457\frac{E_{a\alpha}}{RT_\alpha} \quad (5)$$

Activation energies were evaluated at the conversion levels 8, 12, 16 and 20 %. These levels were chosen since the vast majority of the temperatures derived at the different heating rates for the specific conversion levels were lower than the respective melting points of the complexes, thus precluding the influence of melting on the dissociation kinetics. The plots of log β_α versus the reciprocal temperature values are shown in Fig. 9. Figure 9a and b illustrate fairly linear plots whereas in Fig. 9c the slopes of the plots increase at lower conversion levels, possibly indicating that the process observed is a composite one. For all three complexes the activation energies were calculated by equating the slopes of the curves to $(-0.457E_{a\alpha}/R)$ and solving for $E_{a\alpha}$ (refer to Eq. 5). These values are reported in Table 4 and have been averaged for each sample.

The variation in E_a values obtained for complexes **1** and **2** is random with no trend evident as the conversion level increases. The relative percentage errors for these activation energies are less than 10 %, which is within the conventionally accepted range for isoconversional methods [18]. The decrease in the activation energy for dissociation of complex **3** as a function of α can be explained by the significantly lower melting point of **3** (133 °C) in comparison to complexes **1** (158 °C) and **2** (152 °C); and thus, one, two and three reciprocal temperature values recorded at the 12, 16 and 20 % conversion levels, respectively, were lower than the reciprocal fusion temperature of **3** (see supporting information).

With regard to the activation energies obtained from the isothermal and non-isothermal experiments, the latter are nominally larger; however if their values are examined for

Table 4 Activation energies obtained at specific conversion levels for the three inclusion complexes using non-isothermal thermogravimetric methods

Conversion level (%)	$E_{a\alpha}$ (kJ mol^{-1})		
	1	**2**	**3**
8	142.9	130.1	185.5
12	158.2	155.3	157.8
16	167.7	160.6	138.0
20	166.8	150.4	123.0
Average	158 (12)	149 (13)	151 (27)

each complex, the largest difference in E_a magnitude corresponds to only $\sim$2.5 combined standard deviations. On the other hand, direct comparison of the two sets of activation energies is not strictly justified due to the different methodologies used to obtain them (model-fitting versus model-free/isoconversional methods) and furthermore, the conversion level ranges over which the activation energies were determined were different for the two methods.

We consider the non-isothermal kinetic method as the preferred method to study the complicated systems presented by the three isostructural inclusion complexes since the activation energies calculated from these experiments depend mainly on the initial stages of guest loss, with minimal interference from the process of complex fusion.

Conclusion

The X-ray crystal structures of complexes **2** and **3** provide the first accurate molecular parameters for the guest molecules fenthion and acetochlor. These complexes are also new members of a well-established isostructural TRIMEB inclusion complex series and their addition extends further the already wide variety of guest molecules capable of being included within the host TRIMEB [15]. Furthermore, the present report is the first in which an attempt is made to reconcile kinetic data for the dissociation of guest molecules from permethylated-CD inclusion complexes with the crystal structures of the complexes. There are several studies that have investigated the dissociation of a guest molecule from native CDs [21–23]. The activation energies reported for the thermal dissociation of benzyl alcohol and cinnamaldehyde from their β-CD inclusion complexes, for example, were reported as 158 and 160 kJ mol^{-1} respectively [21, 23], which are very similar to the values of E_a determined here for the three TRIMEB inclusion complexes using the method of non-isothermal TGA. The guest loss process for the β-CD complexes containing benzyl alcohol and cinnamaldehyde occurs via a diffusion-based mechanism, the latter being proposed here as applying also to the TRIMEB inclusion complexes. The dimensionalities of the diffusion-based models are obviously dependent on the packing arrangement of the complex units and are different for the β-CD and TRIMEB complexes discussed here.

It is important to assess the thermal stability of CD inclusion complexes in the solid state. These studies show that a relatively high energy barrier is associated with guest loss from a TRIMEB molecule and that these solid-state complexes should remain intact during normal handling and storage of the material. Finally, the method of mechanical co-grinding employed here, involving a solid host and a guest which is an oil at ambient temperature, may be feasible in an industrial setting to produce large quantities of the complex, thereby stabilising oil-based agrochemicals in a solid form [2].

Supporting information

The CIF files for the complexes **2** and **3** have been deposited with the Cambridge Crystallographic Data Centre (CCDC 857692-857693). These data may be obtained free of charge on request from the CCDC, 12 Union Road, Cambridge CB2 1EZ, UK. Tel.: +44-1233-336408; Fax: +44-1233-336033; E-mail: deposit@ccdc.cam.uk. Additional data: DSC and TG profiles of the co-ground material as well as the computed PXRD patterns generated from the single crystal X-ray structures of the three complexes are supplied. The reciprocal temperature values for the non-isothermal experiments have been tabulated.

Acknowledgments This material is based on research supported by the National Research Foundation (NRF) under Grant number 67381. MRC and DLC express their thanks to the NRF and the University of Cape Town for financial assistance. Financial assistance from Consejo Nacional de Investigaciones Científicas y Técnicas (CONICET), Fondo para la Investigación Científica y Tecnológica (FONCYT), Ministerio de Ciencia y Tecnología (MINCyT), Córdoba (Argentina) and support from the National University of Córdoba are greatly acknowledged. This work was carried out as part of a bilateral cooperation project supported by the NRF (South Africa) and MINCyT (Argentina). NMR is a grateful recipient of a fellowship from CONICET (Argentina).

References

1. Szejtli, J.: Past, present and future of cyclodextrin research. Pure Appl. Chem. **76**, 1825–1845 (2004)
2. Szejtli, J.: Cyclodextrins in pesticides. Starch **37**, 382–386 (1985)
3. Morillo, E.: Applications of cyclodextrins in agrochemistry. In: Dodziuk, H. (ed.) Cyclodextrins and Their Complexes, pp. 459–466. Wiley-VCH Verlag GmBH & Co. KgaA, Weinheim (2006)
4. Kegley, S.E., Hill, B.R., Orne, S.: PAN pesticides database—pesticide registration status. http://www.pesticideinfo.org (2011). Accessed 15 Oct 2011

5. Kamiya, M., Kameyama, K., Ishiwata, S.: Effects of cyclodextrins on photodegradation of organophosphorus pesticides in humic water. Chemosphere **42**, 251–255 (2000)
6. Vico, R.V., Buján, E.I., de Rossi, R.H.J.: Effect of cyclodextrin on the hydrolysis of the pesticide fenitrothion [*O*, *O*-dimethyl *O*-(3-methyl-4-nitrophenyl) phosphorothioate]. Phys. Org. Chem. **15**, 858–862 (2002)
7. Rougier, N.M., Cruickshank, D.L., Vico, R.V., Bourne, S.A., Caira, M.R., Buján, E.I., de Rossi, R.H.: Effect of cyclodextrins on the reactivity of fenitrothion. Carbohydr. Res. **346**, 322–327 (2011)
8. Cruickshank, D.L., Rougier, N.M., Vico, R.V., de Rossi, R.H., Buján, E.I., Bourne, S.A., Caira, M.R.: Solid-state structures and thermal properties of inclusion complexes of the organophosphate insecticide fenitrothion with permethylated cyclodextrins. Carbohydr. Res. **345**, 141–147 (2010)
9. Program SAINT, Version 7.60a, Bruker AXS Inc., Madison, WI, USA (2006)
10. Program SADABS, Version 2008/1, Bruker AXS Inc., Madison, WI, USA (2008)
11. Harata, K., Uekama, K., Otagiri, M., Hirayama, F.: Conformation of permethylated cyclodextrins and the host–guest geometry of their inclusion complexes. J. Inclusion Phenom. Mol. Recognit. Chem. **1**, 279–293 (1984)
12. Mentzafos, D., Mavridis, I.M., Schenk, H.: Crystal structure of the 1:1 complex of heptakis(2,3,6-tri-*O*-methyl)cyclomaltoheptaose (permethylated β-cyclodextrin) with ethyl laurate. Carbohydr. Res. **253**, 39–50 (1994)
13. Sheldrick, G.M.: A short history of SHELX. Acta Crystallogr. Sect. A. **A64**, 112–122 (2008)
14. Song, Z.-W.: 2-Chloro-*N*-chloromethyl-*N*-(2-ethyl-6-methylphenyl)acetamide. Acta Crystallogr. Sect. E. **E64**, o991 (2008)
15. Cambridge Structural Database and Cambridge Structural Database System. Conquest, Version 1.13, Cambridge Crystallographic Data Centre, University Chemical Laboratory: Cambridge, England (2011)
16. Galwey, A.K., Brown, M.E.: Kinetic Background to thermal analysis and calorimetry, Chap. 3. In: Brown, M.E. (ed.) Handbook of Thermal Analysis and Calorimetry, pp. 147–224. Elsevier Science, Amsterdam (1998)
17. Vyazovkin, S., Wight, C.A.: Isothermal and nonisothermal reaction kinetics in solids: in search of ways toward consensus. J. Phys. Chem. A **101**, 8279–8284 (1997)
18. Vyazovkin, S., Wight, C.A.: Isothermal and non-isothermal kinetics of thermally stimulated reactions of solids. Int. Rev. Phys. Chem. **17**, 407–433 (1998)
19. Ozawa, T.: A new method of analysing thermogravimetric data. Bull. Chem. Soc. Jpn. **38**, 1881–1886 (1965)
20. Flynn, J.H., Wall, L.A.: A quick, direct method for the determination of activation energy from thermogravimetric data. J. Polym. Sci. Part B Polym. Lett. **4**, 323–328 (1966)
21. Zhang, N., Li, J.-H., Cheng, Q.-T., Zhu, M.-W.: Kinetic studies on the thermal dissociation of β-cyclodextrin-benzyl alcohol inclusion complex. Thermochim. Acta **235**, 105–116 (1994)
22. Neoh, T.L., Yamauchi, K., Yoshii, H., Furuta, T.: Kinetic study of thermally stimulated dissociation of inclusion complex of 1-methylcyclopropene with α-cyclodextrin by thermal analayis. J. Phys. Chem. B **112**, 15914–15920 (2008)
23. Li, J.-H., Zhang, N., Li, X.-T., Wang, J.-Y., Tian, S.-J.: Kinetic studies on the thermal dissociation of the inclusion complex of β-cyclodextrin with cinnamic aldehyde. J. Therm. Anal. **49**, 1527–1533 (1997)